Arab J Sci Eng (2016) 41:1857–1865
DOI 10.1007/s13369-015-1909-1

RESEARCH ARTICLE - MECHANICAL ENGINEERING

Experimental and Numerical Study of Axial Turbulent Fluid Flow and Heat Transfer in a Rotating Annulus

Jalal M. Jalil[1] · **Abdul-Jabbar Owaid Hanfash**[1] · **Mousa Riyadh Abdul-Mutaleb**[1]

Received: 26 February 2015 / Accepted: 6 October 2015 / Published online: 24 December 2015

Abstract The present work is an experimental and a numerical investigation of the turbulent fluid flow and heat transfer in an annular channel between two concentric cylinders with heated stationary outer cylinder (constant heat flux) and adiabatic rotating inner cylinder. Numerically, the governing equations are discretized in a finite volume fashion using a non-staggered (collocated) arrangement of the variables. The solutions were obtained using the SIMPLE algorithm with upwind scheme. A computer program in FORTRAN 90 was build to solve a set of partial differential equations that govern the fluid flow and heat transfer in annular channels. The experimental results are obtained for an inlet air velocity range of 2–6 m/s, for a wall heat flux range of 600–1200 W/m^2 and a rotational speed range of inner cylinder of 0–1500 rpm with a gap width of 1.5 cm. Finally, the relationships between the average Nusselt number and the effective Reynolds number for experimental and numerical results were proposed and compared with those in the existing literature.

Keywords Effective Reynolds number · Concentric annulus · Turbulent flow · Annulus

List of symbols

d	Air gap thickness or gap width (m): $d = r_o - r_i$
D_h	Hydraulic diameter (m): $D_h = 2(r_o - r_i)$
r_o	Radius of outer cylinder (m)
r_i	Radius of inner cylinder (m)
u_{in}	Inlet air velocity (m/s)
N	Rotation speed of inner cylinder (rpm)
L	Length (m)
k_a	Air thermal conductivity (W/m^2 °C)
q_w	Wall heat flux (W/m^2)
$\overline{T_s}$	Average surface temperature of outer cylinder (°C)
$\overline{T_a}$	Average air temperature (°C)
P	Pressure (N/m^2)
k	Turbulent kinetic energy (m^2/s^2)
$\overline{Nu}$	Average Nusselt number: $\overline{Nu} = q_w D_h/(\overline{T_w} - \overline{T_a})k_a$
Pr	Prandtl number: $\mathrm{Pr} = \mu C_p/k_a$
Re_a	Axial Reynolds number: $Re_a = \rho\ u_{in} D_h/\mu$
Re_r	Rotational Reynolds number: $Re_r = \rho\ r_i \Omega D_h/\mu$
u_{eff}	Effective velocity (m/s): $u_{eff} = [u_{in}^2 + (r_i\Omega/2)^2]^{0.5}$
Re_{eff}	Effective Reynolds number: $Re_{eff} = \rho\ u_{eff} D_h/\mu$

Greek symbols

μ	Dynamic viscosity (N s/m^2)
μ_t	Turbulent viscosity (N s/m^2)
Ω	Angular velocity of inner cylinder (rad/s): $\Omega = 2\pi N/60$
ρ	Density (kg/m^3)
ε	Turbulent energy dissipation rate (m^2/s^2)
Γ	General exchange coefficient

Subscript

a	Axial
r	Rotational
eff	Effective
w	Wall
in	Inlet
t	Turbulent
o	Outer
i	Inner

✉ Jalal M. Jalil
jalalmjalil@gmail.com

[1] Electromechanical Engineering Department, University of Technology, Baghdad, Iraq

1 Introduction

The study of fluid flow and heat transfer in concentric cylinders with rotating inner cylinder is very important in many industrial applications, particularly in electrical, mechanical, chemical and nuclear fields. The applications are electric machines (motors and generators), journal bearing, coaxial rotating heat pipes, axial flow pumps, rotating extractors, combustion chamber, fusions reactors, etc.

Gazley [1] performed an experimental evaluation of the heat transfer in an annular channel in two cases: grooved and un-grooved rotors. The results of these experiments showed that the relation of Nusselt number with effective Reynolds number is: $Nu = Re_{\text{eff}}^{0.8}$. Kuzay [2] studied experimentally the heat transfer of turbulent flow in an annulus channel between two coaxial cylinders with rotating inner cylinder. The surface of the inner cylinder was insulated, and the outer cylinder was fixed and had uniform heat flux. The results showed that Nusselt number of combined flow increased with inner cylinder rotational velocity increase. Pfitzer and Beer [3] presented the effect of rotation of the tubes in an annular flow between two coaxial tubes, on the distribution of velocity, temperature and heat transfer coefficient of the outer cylinder surface. The inner cylinder was assumed insulated and the outer cylinder with uniform heat flux. The results of this study showed that the rotation of inner cylinder affected more than rotation of outer cylinder on Nusselt number of outer cylinder surface. Smyth and Zurita [4] analyzed numerically the axial flow forced convective heat transfer on a rotating cylinder; the results showed that Nusselt number depends on Reynolds number raised to the power 0.8. Escudier and Gouldson [5] experimentally investigated axial, radial and tangential components of velocity and root mean square velocity fluctuations in concentric annular flow for Newtonian and a shear thinning polymer in laminar, transitional and turbulent flow region with a rotating center body of radius ratio 0.506. The results showed that the influence of center body rotation on pressure drop in concentric annular flow is negligible under turbulent flow conditions for both fluids. Char and Hsu [6] conducted a numerical computation for turbulent mixed convection of air in a horizontal concentric annulus between a cooled outer cylinder and a heated, rotating, inner cylinder. The results of this study showed that the average Nusselt number increases with an increase in Rayleigh number, but decreases with an increase in axial Reynolds number and radius ratio. Tzeng [7] experimentally investigated the local heat transfer of a coaxial rotating cylinder. The test rig was designed to make the inner cylinder rotate and the outer cylinder stationary. The inner surface of the inner cylinder was heated with a film heater. The experimental results showed that the heat transfer coefficient increases with rotational Reynolds number increase. Ouali et al. [8] presented an experimental identification technique for the convective heat transfer coefficient inside a rotating cylinder with an axial airflow. It showed that convective exchanges on the internal wall of the cylinder depend on the rotation and the axial air flow. For high rotational speeds, the heat transfer rate is governed by rotation and the axial flow only slightly influences the internal convective heat transfer. Sukumaran and Santhosh [9] investigated the convective heat transfer inside a rotating annulus with an axial air flow. The numerical study was designed to make the inner cylinder rotating and with constant heat flux while the outer cylinder stationary at constant operating temperature. The results showed that rotation has significant effect on heat transfer at lower axial Reynolds number, while for higher axial Reynolds number it was less significant. Ahmadabadi and Karrabi [10] presented an experimental investigation of heat transfer in a non-annular channel between rotor and stator similar to a real generator. The boundary condition assumed a non-homogenous heat flux through the passing air channel. The results showed that the heat transfer coefficient in the axial distribution of stator surface was more uniform than heat transfer coefficient in axial distribution of rotor surface. Fully developed turbulent flow large-eddy simulations in a concentric annulus, $r_i/r_o = 0.5$, $Re_h = 12,500$, with the outer wall rotating was studied by Hadziabdic et al. [11]. Fénot et al. [12] reviewed heat transfer in flow between concentric rotating cylinders which is a long-existing academic and industrial subject (in particular, for electric motors cooling).

Many researchers have investigated the fluid flow and heat transfer in concentric cylinder with rotating inner cylinder, by investigating the effect of heated inner cylinder. However, some recent studies have been carried out concerning heat transfer from a stator (outer cylinder). The present work uses computational fluid dynamics with finite volume to solve the continuity, momentum and energy equations with two dimensional axisymmetric steady flows, with collocated grid. The experimental work was done by building two concentric cylinders similar to practical generator. The constant heat flux is applied on the outer cylinder. The study investigates the turbulent forced convection in a concentric annulus. This study aims at investigating the following parameters: inlet air velocity, rotation speed of rotor and stator heat flux.

2 Physical Model

Figure 1 shows the physical model for concentric annulus. The inner cylinder is rotating with an angular velocity Ω rad/s, and outer cylinder is kept stationary. The inner cylinder is kept in adiabatic condition and outer cylinder wall subjected to constant heat flux. The inlet velocity of the air is uniform u_{in} entering at ambient temperature and exiting through the other side of the annulus.

Fig. 1 Physical model

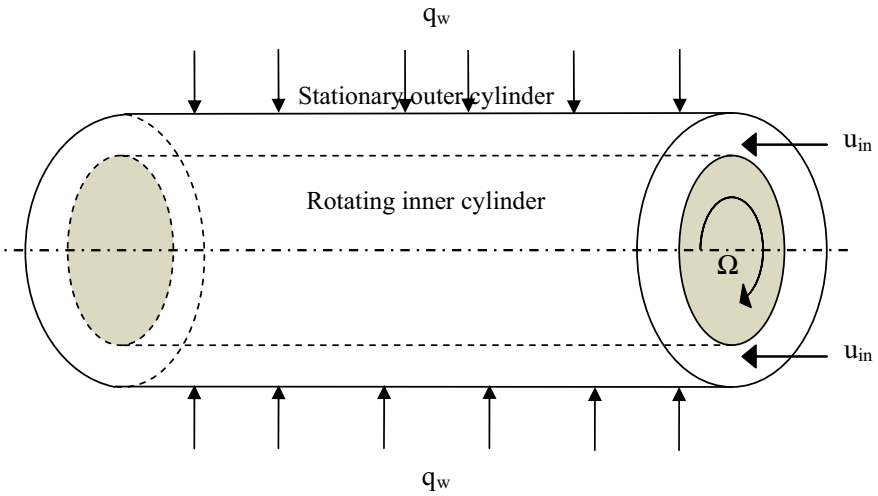

Consider a turbulent forced flow through a concentric annulus consisting of the rotating inner cylinder and heated stationary outer cylinder. It is assume that the flow is steady, incompressible and axi-symmetric. The fluid is assumed to have constant physical properties, and body forces are absent. k-ε turbulence model is used. The equations of continuity, momentum, energy, turbulent kinetic energy (k) and turbulent energy dissipation rate (ε) can be written as follows:
Continuity

$$\frac{\partial u}{\partial z}+\frac{v}{r}+\frac{\partial v}{\partial r}=0 \tag{1}$$

u-momentum

$$u\frac{\partial \rho u}{\partial z}+v\frac{\partial \rho u}{\partial r}=-\frac{\partial p}{\partial z}+\frac{\partial}{\partial z}\left(\mu_{\text{eff}}\frac{\partial u}{\partial z}\right)+\frac{\partial}{\partial r}\left(\mu_{\text{eff}}\frac{\partial u}{\partial r}\right)+\frac{\partial}{\partial z}\left(\mu_{\text{eff}}\frac{\partial u}{\partial z}\right)+\frac{\partial}{\partial r}\left(\mu_{\text{eff}}\frac{\partial v}{\partial z}\right) \tag{2}$$

v-momentum

$$u\frac{\partial \rho v}{\partial z}+v\frac{\partial \rho v}{\partial r}=-\frac{\partial p}{\partial r}+\frac{\partial}{\partial z}\left(\mu_{\text{eff}}\frac{\partial v}{\partial z}\right)+\frac{\partial}{\partial r}\left(\mu_{\text{eff}}\frac{\partial v}{\partial r}\right)\frac{\partial}{\partial z}\left(\mu_{\text{eff}}\frac{\partial u}{\partial r}\right)+\frac{\partial}{\partial r}\left(\mu_{\text{eff}}\frac{\partial v}{\partial r}\right)+\rho\frac{w^2}{r}-\mu_{\text{eff}}\frac{v}{r^2} \tag{3}$$

w-momentum

$$u\frac{\partial \rho w}{\partial z}+v\frac{\partial \rho w}{\partial r}=\frac{\partial}{\partial z}\left(\mu_{\text{eff}}\frac{\partial w}{\partial z}\right)+\frac{\partial}{\partial r}\left(\mu_{\text{eff}}\frac{\partial w}{\partial r}\right)+\rho\frac{vw}{r}-\mu_{\text{eff}}\frac{w}{r^2} \tag{4}$$

Table 1 Grid independency

Grids in (z, r)	$\overline{Nu}$
(22, 58)	29.61
(35, 83)	29.80
(51, 101)	30.06
(58, 110)	30.32
(69, 116)	30.37
(81, 138)	30.37

Energy

$$u\frac{\partial \rho T}{\partial z}+v\frac{\partial \rho T}{\partial r}=\frac{\partial}{\partial z}\left(\Gamma_{\text{eff}}\frac{\partial T}{\partial z}\right)+\frac{\partial}{\partial r}\left(\Gamma_{\text{eff}}\frac{\partial T}{\partial r}\right) \tag{5}$$

where the effective viscosity coefficient (μ_{eff}) equals to $\mu_{\text{eff}} = \mu + \mu_{\text{t}}$. Then, the turbulent viscosity (μ_{t}) is obtained as $\mu_{\text{t}} = \frac{\rho C_\mu k^2}{\varepsilon}$. Whereas, the effective exchange coefficient is calculated as $\Gamma_{\text{eff}} = \frac{\mu}{Pr} + \frac{\mu_{\text{t}}}{Pr_{\text{t}}}$.
k-equation

$$u\frac{\partial \rho k}{\partial z}+v\frac{\partial \rho k}{\partial r}=\frac{\partial}{\partial z}\left(\Gamma_{\text{eff}}\frac{\partial k}{\partial z}\right)+\frac{\partial}{\partial r}\left(\Gamma_{\text{eff}}\frac{\partial k}{\partial r}\right)+G-\rho\varepsilon \tag{6}$$

ε-equation

$$u\frac{\partial \rho \varepsilon}{\partial z}+v\frac{\partial \rho \varepsilon}{\partial r}=\frac{\partial}{\partial z}\left(\Gamma_{\text{eff}}\frac{\partial \varepsilon}{\partial z}\right)+\frac{\partial}{\partial r}\left(\Gamma_{\text{eff}}\frac{\partial \varepsilon}{\partial r}\right)+C_1G\frac{\varepsilon}{k}-C_2G\frac{\varepsilon^2}{k} \tag{7}$$

Here, G is the generation term, which according to the standard k-ε model is given by [13]:

$$G = \mu_t \left\{ 2\left[\left(\frac{\partial u}{\partial z}\right)^2 + 2\left(\frac{\partial v}{\partial r}\right)^2 + \left(\frac{v}{r}\right)^2 \right] + \left(\frac{\partial u}{\partial r} + \frac{\partial v}{\partial z}\right)^2 + \left(\frac{\partial w}{\partial r} - \frac{w}{r}\right)^2 \right\} \quad (8)$$

The values of the empirical constants used in the standard k-ε model are given below [13]:

$$C_1 = 1.44,\ C_2 = 1.92,\ C_\mu = 0.09,\ Pr_{t,k} = 1.0,\ Pr_{t,\varepsilon} = 1.3.$$

The governing equations are discretized in a finite volume fashion using a non-staggered (collocated) arrangement of the variables. The solutions were obtained using the SIMPLE algorithm with upwind scheme. A computer program in FORTRAN 90 is written to solve a set of the partial differential equations that govern the fluid flow and heat transfer in annular channel. To eliminate the errors due to coarseness of grid, analysis has been carried out for different number of nodes in the annulus for gap width of 1.5 cm. Grid independence study is carried out in heat transfer through annular gap for inlet air velocity 3 m/s, and heat flux 1200 W/m^2, without rotation. The variation of average Nusselt number with number of nodes in z and r directions is shown in Table 1. The suitable number of nodes for this study is (69,116) in (z and r) directions, respectively.

3 Experimental Apparatus

Figure 2 is a schematic diagram of the experimental apparatus. A photograph that presents the experimental apparatus is shown in Fig. 3. As seen, the blower supplies the air through pipe and reducer like contraction to provide fairly uniform flow with minimum turbulence intensity in the test section inlet. To alternate the path of air flow, a pyramidal form and then mesh were used. Two pulleys are used for conveying power between the electric motor and test section rotor.

Three electric heaters of 1200 W are attached to the outer surface of the outer cylinder (stator). Figure 4 shows test section and thermocouple positions. The rotor consists of an inner cylinder of iron material, with length of 34 cm and diameter of 20 cm. The stator is composed of an outer cylinder of iron material, with length of rotor, inner diameter of 23 cm and outer diameter 23.9 cm. The ratio of the two diameters and ratio of length to the thickness of air gap are $D_i/D_o = 0.869$ and $L/d = 22.66$, respectively. Mica-thermal insulation is used to reduce the heat loss to ambient from heaters. Chromel-Alumel thermocouple wires type K with precision of $\pm 1\,^\circ$C is used to measure the temperatures. Six thermocouples are used to measure the temperature surface of stator, while eight thermocouples are used to measure the temperature of air in air gap, and one thermocouple is used to measure the temperature on the insulator to calculate heat loss to the surround. Thermocouple sensors were fixed to the

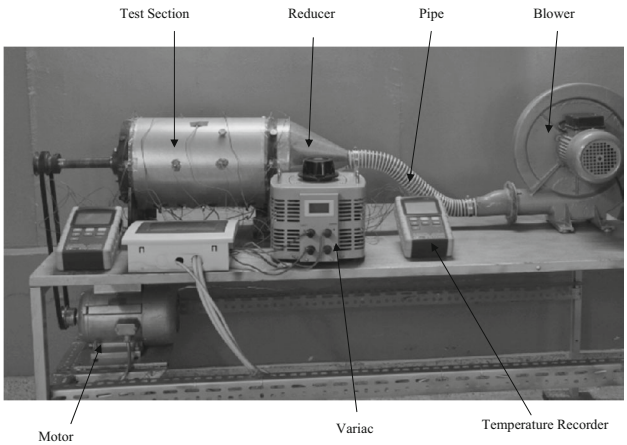

Fig. 3 Photograph picture of experimental apparatus

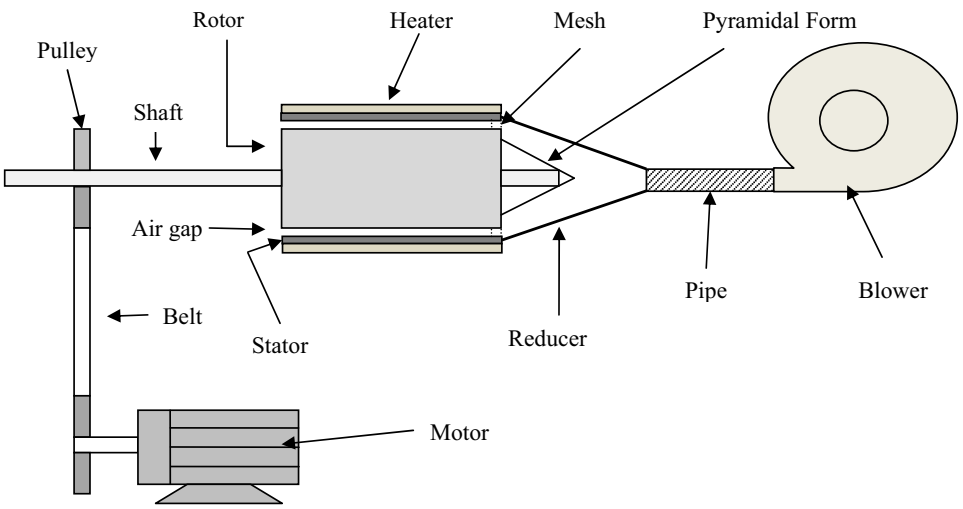

Fig. 2 Schematic representation of experimental apparatus

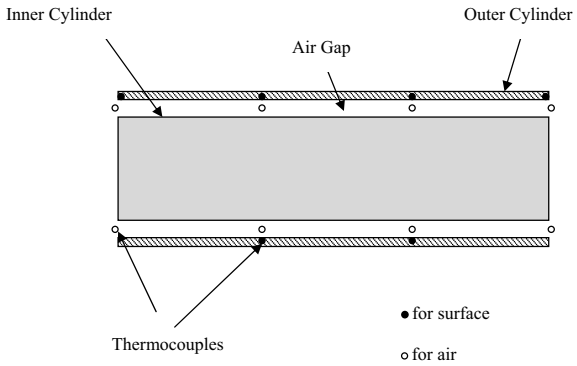

Fig. 4 Test section and thermocouple positions

surface of the tested channel via isolated thermal glue material. The choice of this material takes into considerations hot conduction small bore of size less than sensor size was made to prevent the movement of the thermocouples. The thermocouple sensors measure the stator surface and air temperature by using 12-channel digital temperature recorder.

Variac is used for varying the voltage of the three heaters on the stator in order to vary the heater power for each test. Digital power clamp meter is used for power measurement. The air velocity in the air gap is measured by hot wire anemometer, and to adjust the mass flow rate of blower, a mechanical gate is used. To change the speed of rotor, three sizes of pulleys were used. Digital laser tachometer is used to measure rotation speed of rotor.

Consider the hydraulic diameter D_h as characteristic length in dimensionless calculation; the axial Reynolds number is obtained as:

$$Re_a = \frac{\rho u_{in} D_h}{\mu}, \tag{9}$$

while the rotational Reynolds number is calculated as:

$$Re_r = \frac{\rho r_i \Omega D_h}{\mu} \tag{10}$$

Now, the effective Reynolds number which is a combination of axial and rotational Reynolds numbers is written as:

$$Re_{eff} = \frac{\rho D_h \left(u_{in}^2 + \alpha (r_i \Omega)^2\right)^{1/2}}{\mu} \tag{11}$$

where α is a coefficient taking into account the influence of rotor speed compared to influence of inlet velocity. $\alpha = 0.25$ is used in the numerical and experimental calculations.

The average Nusselt number can be calculated as:

$$\overline{Nu} = \frac{q_w D_h}{\left(\overline{T_s} - \overline{T_a}\right) k_a}$$

where $\overline{T_s}$ is the average surface temperature of outer cylinder and $\overline{T_a}$ is average air temperature.

4 Results and Discussion

Figure 5 shows the variation of average internal surface temperature of outer cylinder with inlet air velocity at different rotation speeds of inner cylinder and at a heat flux of 900 W/m^2. The surface temperature decreases as the inlet air velocity increases from 2 to 6 m/s, because forced convection removes heat from the surface of outer cylinder. Figure 6 illustrates the variation of surface temperature of outer cylinder with heat flux for various inlet air velocities without rotation. It can be noticed that surface temperature increased as the heat flux increased from 600 to 1200 W/m^2.

Figure 7 illustrates the increase in the average Nusselt number with increase in the axial Reynolds number. In the case of higher axial Reynolds number, the rotational Reynolds number has less significance effect; this is due to higher axial velocity compared with rotational velocity.

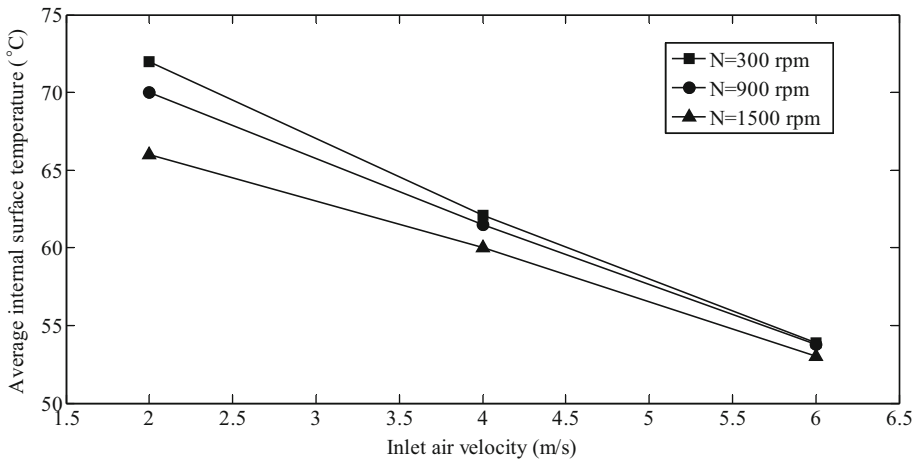

Fig. 5 Variation of average internal surface temperature of outer cylinder with inlet air velocity for various rotation speed and for $q_w = 900$ W/m^2

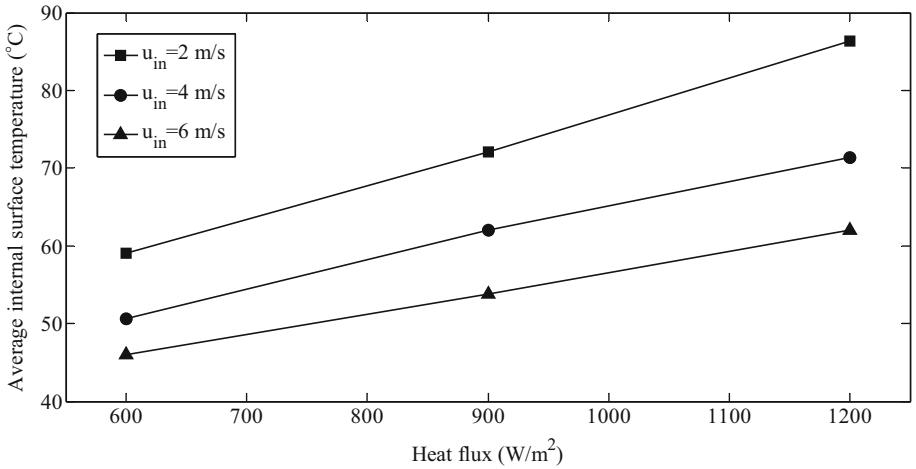

Fig. 6 Variation of average internal surface temperature of outer cylinder with heat flux for different values of inlet air velocity without rotation

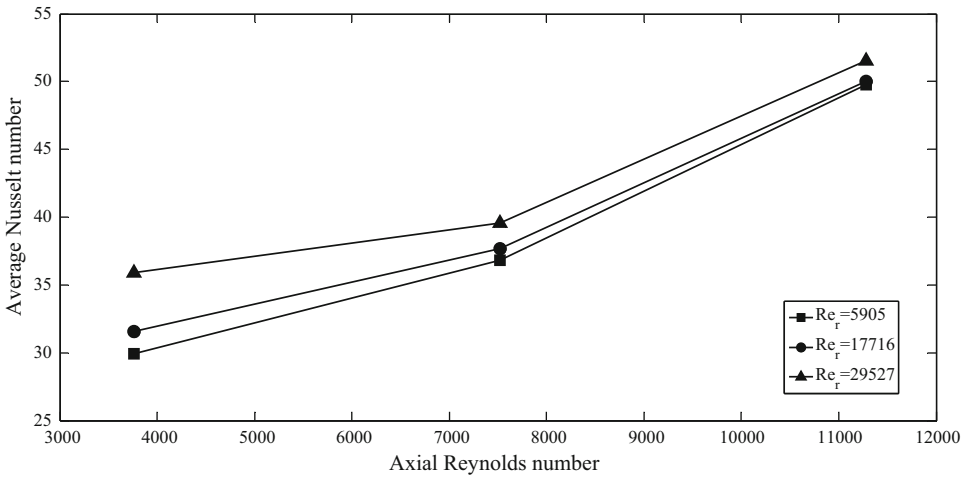

Fig. 7 Variation of average Nusselt number with axial Reynolds number for various rotational Reynolds number and for $q_w = 900\,\mathrm{W/m^2}$

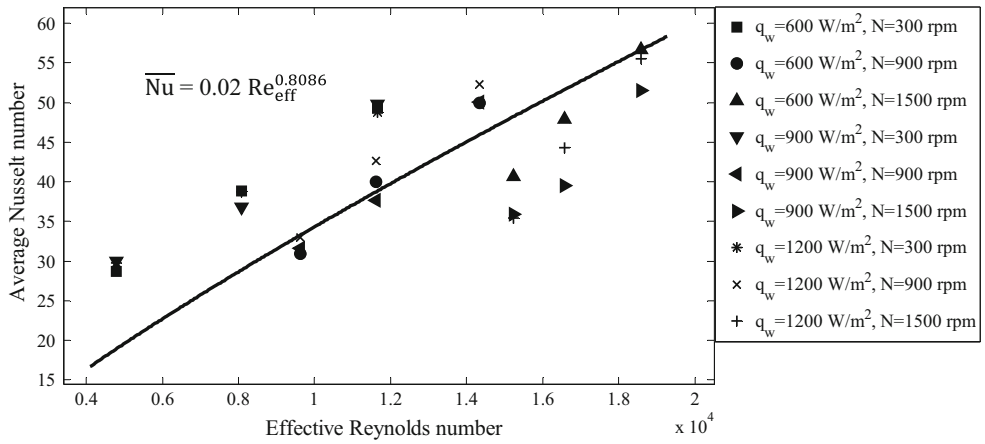

Fig. 8 Variation of average Nusselt number with effective Reynolds number for different heat flux

Figure 8 shows the variation of average Nusselt number with effective Reynolds number at different inner cylinder rotation speed at various heat fluxes. The relation between average Nusselt number and effective Reynolds number is formulated as $\overline{Nu} = 0.02 Re_{\mathrm{eff}}^{0.8066}$ for $4700 < Re_{\mathrm{eff}} < 18{,}600$.

Figure 9 shows the change in average internal outer cylinder temperature with inner cylinder rotation at different inlet air velocities and at heat flux of $1200\,\mathrm{W/m^2}$ and gap width 0.5 cm. It is obvious that the increase in inlet air velocity reduces the average internal outer cylinder surface temperature with constant heat flux, but for

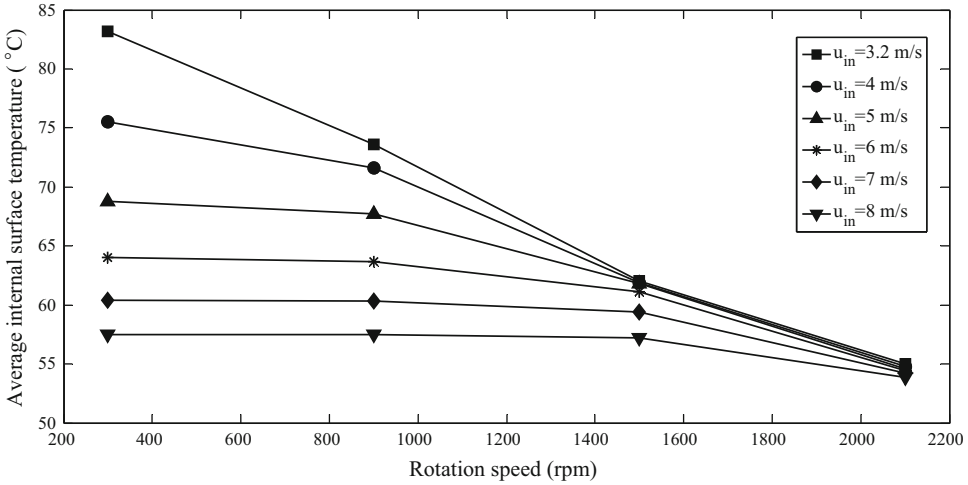

Fig. 9 Variation of average internal surface temperature of outer cylinder with rotation speed at different air velocity and for $q_w = 1200\,W/m^2$ gap width 0.5 cm

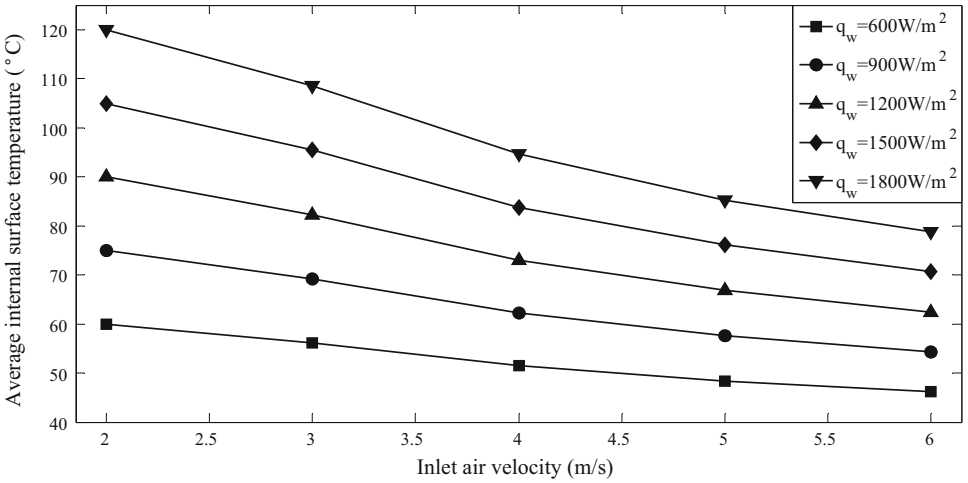

Fig. 10 Variation of average internal surface temperature of outer cylinder with inlet air velocity at different heat flux and at gap width 1.5 cm without rotation

rotation speed larger than 1400 rpm, the effect is reduced or diminished. The reason for this behavior is the narrow gap width; the rotational velocity has higher effect than the axial velocity. Figure 10 shows the variation of average internal outer cylinder temperature with inlet air velocity for various heat fluxes and at gap width of 1.5 cm without rotation. This figure reveals that the surface temperature increases as the heat flux increases from 600 to 1800 W/m^2.

Figure 11 shows the change in average Nusselt number with axial Reynolds number at different rotational Reynolds number, at heat flux 600 W/m^2 and gap width 1.5 cm. The average Nusselt number increases with axial Reynolds number increases from 3761 to 11,284. As shown in Fig. 11, as the rotational Reynolds number increases, the average Nusselt number increases at low axial Reynolds number. At high axial Reynolds number, the effect of rotational Reynolds number is reduced or diminished. Figure 12 shows the variation of average Nusselt number with effective Reynolds number at different rotation speeds of inner cylinder and at various heat fluxes. The relation between average Nusselt number and effective Reynolds number is formulated as $\overline{Nu} = 0.02\,Re_{\text{eff}}^{0.7835}$ for $4700 < Re_{\text{eff}} < 23,600$.

Figure 13 shows the isothermal distribution in annular gap for gap thickness 1.5 cm, heat flux 1200 W/m^2 and inlet air velocity 2 m/s without rotation. The temperature begins to increase at axial direction (stream-wise direction), while at radial direction, the temperature begins to decrease from the wall of outer cylinder toward the air gap center. The temperature is maximum at the wall of outer cylinder.

Figure 14 shows the comparison between the numerical and experimental results for variation of average internal outer cylinder temperature with rotation at heat flux 900 W/m^2 and inlet air velocity 4 m/s. It shows a good agreement between the numerical and experimental results. Figure 15 shows a comparison between the present numerical and experimental results correlation with the experimental results of Gazley [1], $\overline{Nu} = 0.022 Re_{\text{eff}}^{0.8}$, based on $\alpha = 0.25$. Ahmadabadi and Karrabi [10] found that the relation between average Nusselt number with effective

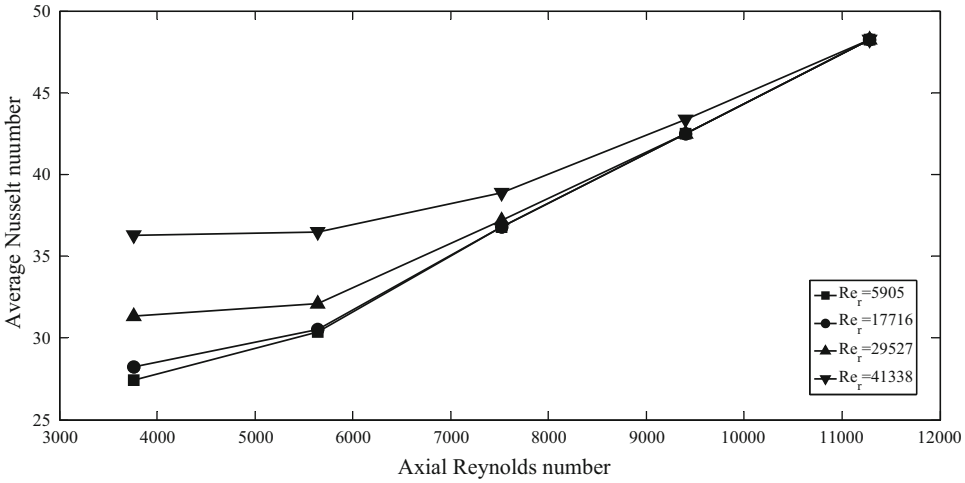

Fig. 11 Variation of average Nusselt number with axial Reynolds number for various rotational Reynolds number and for $q_w = 600\,W/m^2$ at gap width 1.5 cm

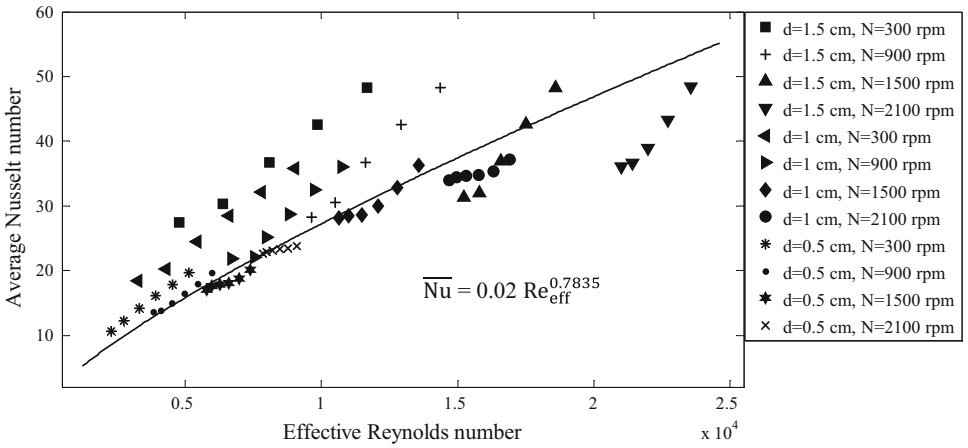

Fig. 12 Variation of average Nusselt number with effective Reynolds number at various gap widths

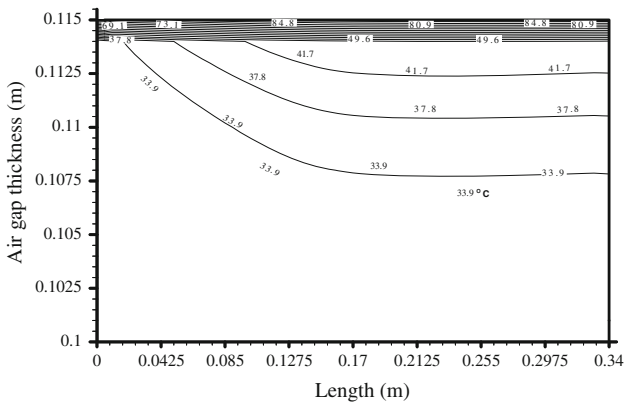

Fig. 13 Isothermal distribution in annular gap for $q_w = 1200\,W/m^2$ and for $u_{in} = 2\,m/s$ without rotation at gap width 1.5 cm

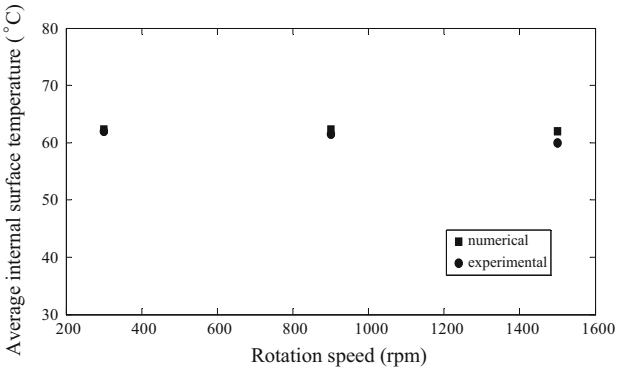

Fig. 14 Comparison between numerical and experimental results for variation of average internal surface temperature of outer cylinder with rotation speed at $q_w = 900\,W/m^2$ and for $u_{in} = 4\,m/s$

Reynolds number correlated as $\overline{Nu} = 0.0202\,Re_{eff}^{0.8359}$, based on $\alpha = 0.25$. The relation between average Nusselt number and effective Reynolds number for experimental and numerical results correlated as $\overline{Nu} = 0.02\,Re_{eff}^{0.7927}$ for $2200 < Re_{eff} < 23,600$. It shows that the present results have remarkable agreement with the Gazley [1] results.

5 Conclusions

From the experimental and numerical results, the following conclusions can be drawn:

1. At high heat flux, the increase in inlet velocity has more effect on decreasing surface temperature.

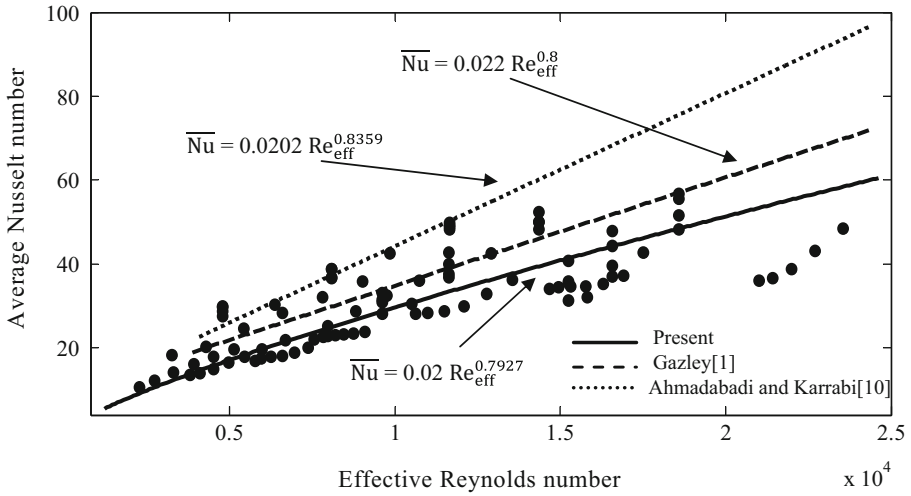

Fig. 15 Comparison of the experimental and numerical results with existing literature

2. At wide gap (1.5 cm), when rotational Reynolds number increases, the Nusselt number increases. But at high axial Reynolds number, the effect of the rotation is minimized or diminished.
3. At narrow gap width (0.5 cm), the rotational velocity dominated and the effect of inlet velocity is reduced or diminished.
4. The relation between average Nusselt number and effective Reynolds number is formulated as $\overline{Nu} = 0.02\ Re_{\text{eff}}^{0.7927}$.
5. The results show good agreement between experimental and numerical results, and with existing literature.

References

1. Gazley, C.: Heat transfer characteristics of the rotation and axial flow between concentric cylinders. J. Heat Transf. **80**, 79–90 (1985)
2. Kuzay, T.M.: Turbulent heat and momentum transfer studies, Ph.D. Thesis, University of Minnesota, (1973)
3. Pfitzer, H.; Beer, H.: Heat Transfer in an annulus between independently rotating tubes with turbulent axial flow. Int. J. Heat Mass Transf. **35**, 623–633 (1992)
4. Smyth, R.; Zurita, P.: Heat transfer at the outer surface of a rotating cylinder in the presence of axial flow, Trans. Eng. Sci. 5 (1994)
5. Escudier, M.P.; Gouldson, I.W.: Concentric annular flow with center body rotation of a Newtonian and a shear- thinning liquid. Int. J. Heat Fluid Flow **16**, 156–162 (1995)
6. Char, M.I.; Hsu, Y.H.: Numerical prediction of turbulent mixed convection in a concentric horizontal rotating annulus with low-re two-equation models. Int. J. of Heat and Mass Transfer, **41**, 1633–1643 (1998)
7. Tzeng, S.C.: Heat transfer in a Small Gap between Co-Axial Rotating Cylinders. Int. Commun. Heat Mass Transf. **33**, 737–743 (2006)
8. Ouali, S.S.; Saury, D.; Harmand, S.; Laloy, O.: Convective heat transfer inside a rotating cylinder with an axial air flow. Int. J. Therm. Sci. **45**, 1166–1178 (2006)
9. Sukumaran, A.K.; Santhosh, K.S.: Numerical simulation of heat transfer and fluid flow in rotating annulus, In: National Conference on Technological Trends, (2009)
10. Nili-Ahmadabadi, M.; Karrabi, H.: Heat transfer and flow region characteristics study in a non-annular channel between rotor and stator. Therm. Sci. **16**, 593–603 (2012)
11. Hadziabdic, M.; Hanjalic, K.; Mullyadzhanov, R.: LES of turbulent flow in a concentric annulus with rotating outer wall. Int. J.Heat Fluid Flow **43**, 74–84 (2013)
12. Fénot, M.; Bertin, Y.; Dorignac, E.; Lalizel, G.: A review of heat transfers between concentric rotating cylinders with or without axial flow. Int. J. Therm. Sci. **50**, 1138–1155 (2011)
13. Launder, B.E.; Spalding, D.B.: The numerical computation of turbulent flow. Comp. Methods Appl. Mech. Eng. **3**, 269 (1974)